

The structures of small cationic gas-phase platinum clusters

Dan J. Harding,¹ Christian Kerpel,¹ David M. Rayner,² and André Fielicke^{1, a)}

¹⁾*Fritz-Haber-Institut der Max-Planck-Gesellschaft, Faradayweg 4-6, D-14195 Berlin, Germany*

²⁾*National Research Council of Canada, 100 Sussex Drive, Ottawa, Ontario, Canada K1A 0R6*

(Dated: 19 April 2013)

The structures of small platinum clusters Pt_{3-5}^+ are determined using far-infrared multiple photon dissociation spectroscopy of their argon complexes combined with density functional theory calculations. The clusters are found to have compact structures, and Pt_4^+ and Pt_5^+ already favor three dimensional geometries, in contrast to a number of earlier predictions. Challenges in applying density functional theory to 3rd row transition metal clusters are addressed. Preliminary calculations suggest that the effects of spin-orbit coupling do not change the favoured lowest-energy isomers.

Gas-phase clusters are promising model systems to help unravel the complex atomistic details of reactions occurring on real heterogeneous nano-catalysts, including the effects on the reactivity of particle size, shape or charge state. Determination of gas-phase cluster geometric and electronic structures is an important step towards this understanding, demonstrated by the recent interest in the structures of gold clusters.¹⁻⁴ In contrast, despite platinum being much more widely used in catalysis than gold, there are no structural or spectroscopic characterizations of platinum clusters larger than the trimer. There have been significant theoretical efforts to investigate the structures of isolated platinum clusters,⁵⁻¹¹ but so far these are inconclusive, predicting different low-energy structures. Here, we present a combined experimental and computational study of small platinum clusters to determine the structures of Pt_n^+ ($n=3-5$) and investigate what level of theory is necessary to treat these systems reliably.

The importance of platinum in catalysis has led to gas-phase platinum clusters being the subject of a number of experiments to probe their reactivity,¹²⁻¹⁹ which has been found to depend sensitively on cluster size and charge state. Little spectroscopic work has been undertaken on unsupported platinum clusters, though features consistent with two vibrational progressions, at 105 ± 30 and $225 \pm 30 \text{ cm}^{-1}$, have been observed in the photoelectron spectrum of Pt_3^- .²⁰

Practical quantum chemical calculations of the structures and properties of metal clusters remain limited to density functional theory (DFT) for all but the smallest sizes. In many cases, DFT provides accurate results at reasonable computational costs but, because of the approximations introduced in many exchange-correlation functionals, it is necessary to test the results of DFT calculations against experimental results. Vibrational spectroscopy provides an ideal comparison, as it is sensitive to the overall shape and structure of the cluster and the strengths and force constants of the bonds. Additionally,

vibrational spectra can be calculated without knowledge of the excited electronic states of the cluster.

For heavy elements, such as Pt, relativistic effects can become important, influencing both the structure of their compounds and their chemistry. Consequently, these effects may need to be included to provide an accurate theoretical/computational description of the cluster. While the most important relativistic effects can be routinely treated by scalar relativistic effective core potentials (ECP) other effects, particularly spin-orbit coupling (SOC), are more challenging. Several groups have made predictions of Pt cluster structures using DFT⁵⁻¹¹ and post-Hartree-Fock methods²¹⁻²³, with and without the inclusion of SOC. Błoński *et al.*¹⁰ have summarized the available theoretical data on small Pt clusters and there is no consensus as to the favoured structures, with a range of 2- and 3-dimensional isomers proposed, or of the importance of SOC on the favoured isomer. The relative energy differences reported for the different isomers are, in many cases, extremely small. Consequently, only small changes in the energies of the different isomers are needed to change their energetic ordering.

Vibrational spectra of the clusters were obtained in the range from $90-250 \text{ cm}^{-1}$ by far-infrared multiple photon dissociation (FIR-MPD) spectroscopy using the messenger-atom technique. The experimental details and data analysis have been described in detail previously.^{24,25} Briefly, argon-tagged platinum clusters were formed in a laser ablation cluster source using a mixture of argon (0.25 %) in helium. The thermalisation channel of the source was cooled to 148 K. After expansion into vacuum and passage through a skimmer, the ion beam enters the extraction region of a reflectron time-of-flight mass spectrometer. Intense, tunable far-infrared radiation from the Free Electron Laser for Infrared eXperiments²⁶ (FELIX) counterpropagates along the cluster beam, typical providing 20 mJ in a 10 μs long macropulse with a bandwidth of *ca.* 1% fwhm of the central wavelength. When the IR radiation is resonant with a vibrational transition in the cluster multiple photons can be absorbed, heating the cluster, leading to dissociation. Changes in the mass spectrum are monitored as a function of FELIX wavelength. The IR spectra are

^{a)}Electronic mail: fielicke@fhi-berlin.mpg.de

shown on a cross section scale (see Ref.²⁵ for details).

Argon sticks relatively strongly to these small platinum clusters and we can form and detect complexes even with the source at room temperature. The experimentally observed lifetime of the complexes of at least 100 μs sets an upper limit on the unimolecular dissociation rate of 10^4 s^{-1} . From the source temperature and the dissociation rate, using RiceRamspergerKasselMarcus (RRKM) theory we estimate the binding energy of the first Ar atom to be around 0.5 eV. A consequence of the strong binding is that the singly and doubly tagged complexes could not be dissociated. Instead, a higher concentration of argon was used and depletion of the complexes with four or five argon atoms was monitored. The tagging atoms necessary for the messenger-atom technique are usually assumed to cause only small changes to the vibrational spectra of the underlying molecule. When this is the case, the calculations needed for comparison can be performed without inclusion of the tagging atoms. Here, the relatively strongly bound Ar atoms may have a significant effect on the vibrational spectrum of the cluster complex and must therefore be explicitly included in the calculations.

DFT calculations for bare and Ar-tagged Pt clusters were carried out using the TPSS exchange-correlation functional²⁷ with the def2-TZVP ECP and basis sets^{28,29} using TURBOMOLE 6.0.³⁰ To investigate the effects of SOC we have performed calculations using NWChem 6.0,³¹ with the TPSS functional²⁷ and the CRENL ECP, basis set and SO potential,³² which allows local optimization and frequency calculations with and without SOC. Currently, SOC calculations in NWChem cannot be performed with symmetry and IR intensities are not available, making the comparison with our experimental data more complicated. The results of the calculations for the bare clusters are shown in the supplementary material.³³

A range of different geometries and spin-multiplicities³⁴ were considered for each cluster size, the low-energy isomers were then decorated with argon and these structures reoptimised followed by frequency calculations. The frequencies are not scaled. As the clusters are charged, the most important interactions between the cluster and the Ar atoms are expected to be charge induced-dipole, rather than the non-local dispersion forces which are not treated by DFT.

Figure 1 shows the experimental FIR-MPD spectra and comparison with the calculated spectra for the Ar complexes of clusters containing three platinum atoms. Pt_3Ar_5^+ has two intense bands at 98 and 111 cm^{-1} and a weak feature at 145 cm^{-1} . Monitoring the Pt_3Ar_2^+ channel, the lowest Ar-coverage for which we see IR-induced intensity changes, we observe growth at 114 and 142 cm^{-1} due to fragmentation of $\text{Pt}_3\text{Ar}_{3-5}^+$. This growth, which appears as an apparent negative cross section, provides a composite spectrum for the clusters with higher Ar-coverage.

The bare Pt_3^+ cluster, despite its small size, presents a

TABLE I. Calculated properties for triangular isomers of Pt_3^+ clusters at different levels of theory.

$2s + 1$	E/Hartrees	$\Delta E/\text{eV}$	Frequencies/ cm^{-1}
TPSS/def2-TZVP			
2	-357.683821	0.00	148, 165, 229
4	-357.680889	0.08	145, 146, 219
6	-357.625307	1.59	65, 138, 219
TPSS/CRENL			
2	-358.521039	0.12	121, 121, 250
4	-358.525477	0.00	154, 167, 237
6	-358.475738	1.35	128, 146, 234
TPSS/CRENL with SOC			
2	-358.915055	0.03	144, 149, 228
4	-358.916141	0.00	134, 143, 233
6	-358.916128	0.00	130, 200, 222

challenge to theory. The three levels of theory we have investigated, shown in Table I, all favour triangular structures but do not agree on the symmetries and spin multiplicities. We have also investigated linear isomers, but found them to be higher in energy and, in many cases, saddle points. The calculated frequencies of the doublet and quartet triangular isomers are all fairly similar, with one mode of low or zero IR intensity above 220 cm^{-1} , and two close (or degenerate) modes somewhere between 130 and 170 cm^{-1} . As the band(s) observed in the experiment below 120 cm^{-1} are due to the Ar-tagging, the band at 142 cm^{-1} is the most useful for comparison with calculations of the bare clusters. Several of the spectra calculated for the triangular structures provide a reasonable match to the position of this band, the best is provided by a doublet calculated with the inclusion of SOC, with modes at 144 and 149 cm^{-1} . Unfortunately, similar changes in the calculated frequencies are caused by changes in ECP/basis set, spin multiplicity or geometry which, combined with the small energy differences and the complication of the Ar-tagging atoms, makes it difficult to distinguish between equilateral or lower symmetry triangles or doublet or quartet electronic states.

The spectra calculated with explicit inclusion of the Ar tagging atoms provide qualitatively good matches to the experiment, particularly to the growth seen in the Pt_3Ar_2^+ channel. The frequencies around 150–170 cm^{-1} are due to metal-metal modes, while the intense low frequency bands are due to asymmetric Ar-cluster-Ar stretches. The band at 99 cm^{-1} is not reproduced by the harmonic spectra, even when taking the argon atoms into consideration. Given this problem, and the fact that some of the argon covered clusters have small imaginary frequencies (*ca.* 10 cm^{-1}) where we have been unable to find true local minima due to the extremely flat nature of the potential energy surface, we have used Molecular Dynamics simulation with the FHI-AIMS program³⁵, described in the supplementary material, to investigate possible effects of anharmonicity or dynamics. For the $^4\text{Pt}_3\text{Ar}_5^+$, the resulting spectrum, shown in Fig 1, is similar to the harmonic spectrum, with the exception of

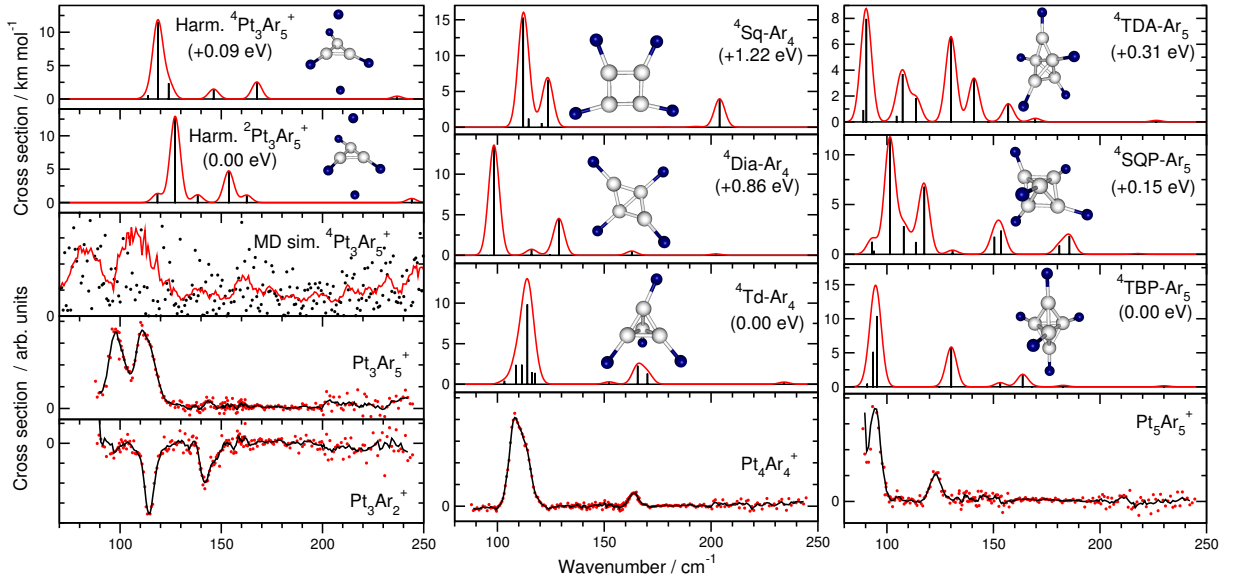


FIG. 1. Experimental and calculated spectra of $Pt_n Ar_m^+$. (a) $Pt_3 Ar_m^+$; the experimental spectrum of $Pt_3 Ar_2^+$ shows growth due to fragmentation of clusters with more argon, below *ca.* 100 cm^{-1} the heating of the clusters appears to be insufficient to boil off three Ar atoms from $Pt_3 Ar_5^+$, (b) $Pt_4 Ar_4^+$ and (c) $Pt_5 Ar_5^+$. All of the harmonic spectra were calculated at the TPSS/def2-TZVP level, the relative energies are shown for the argon complexes. The leading superscripts show the spin multiplicity of the species.

a second low-frequency band. Though this position of this feature does not match the experiment perfectly, it strongly suggests that the feature at 99 cm^{-1} is due to dynamic effects in the argon complex which cannot be described by the stationary harmonic spectra.

The experimental spectrum of $Pt_4 Ar_4^+$, shown in Figure 1, has two features, at 110 and 164 cm^{-1} . Both SOC and non-SOC calculations favour (roughly) tetrahedral (Td) geometries for the bare Pt_4^+ clusters. The calculated spectra of these low-energy structures provide a good match to the band positions of the experimental spectrum. If the argon atoms are included in the calculation, shown in Fig. 1, the intensities also match well. In this case, unlike $Pt_3 Ar_n^+$, the bands at *ca.* 110 cm^{-1} are not due solely to Pt-Ar modes but, at least in part, to metal-metal modes. While all three methods we have used find similar lowest-energy structures, the energy order and stability of other isomers are different. However, none of these isomers provide such a good match to the experimental spectrum. The most intense IR bands for the square (Sq) isomers are in the $190\text{-}200 \text{ cm}^{-1}$ region, for the diamond (Dia) isomers they are more variable but they do not have intense features around 160 cm^{-1} . In the case of the SOC calculations, the square isomers are all found to be transition states, while the diamond isomers collapse to Td structures during optimisation.

For bare Pt_5^+ clusters, we find quartet states of the square pyramid (SQP) and trigonal bipyramid (TBP) isomers to be basically isoenergetic at all three levels of calculation. The next best isomer, a tetrahedron with a bridge-bound adatom (TDA), is also relatively close in energy, from 0.05 to 0.2 eV depending on the level of

theory. We have also investigated several planar isomers, but found these to be higher in energy (0.5 eV). There are slightly larger differences in relative energies between the TPSS/CRENBL calculations with and without SOC than between the two sets of calculations without SOC (TPSS/CRENBL and TPSS/def2-TZVP) *i.e.* SOC appears to have a larger effect than the change of ECP and basis sets.

Including the Ar-atoms for the quartet states we find slightly larger energy differences than for the bare clusters, with $^4\text{TBP-Ar}_5$ now 0.15 eV lower in energy than $^4\text{SQP-Ar}_5$. Comparison of the experimental and calculated spectra, shown in Fig. 1, finds a much better match for the $^4\text{TBP-Ar}_5$ than for the other isomers, matching the positions of the intense peaks at <95 and 123 cm^{-1} . The small band at 165 cm^{-1} in the calculated spectrum is probably too weak for us to observe. The other calculated spectra do not provide good matches as they have too many features.

Given the very small energy differences predicted for at least three isomers of Pt_5^+ it is surprising that we observe only one isomer, though the small number of features in the experimental spectrum also supports this interpretation. There are several possible reasons why this might be the case including i) argon may stick preferentially to the TBP isomer, ii) argon adsorption may lead to rearrangement of other isomers to the TBP, iii) the DFT energy differences are too small and the TBP is significantly lower in energy than the other isomers.

The structures we have identified for Pt_{3-5}^+ are simple, close-packed geometries. They are similar to the structures we have identified for clusters of other transi-

tion metals.^{36,37} This is in agreement with structures predicted for the neutral clusters by post-Hartree-Fock^{21–23} and some^{5,7,9,11} of the DFT calculations. One possible (physical) source of difference is the charge state of the clusters, as our experiments and calculations are on cationic clusters, while the previous computational studies have investigated neutrals. For gold clusters, different charge states are known to favour different isomers^{1,3,4} and the transition from 2D to 3D isomers is observed at significantly smaller sizes for the cations than the anions. The adsorption of the Ar tagging atoms may also influence the observed isomer, though we have found no cases where the favored isomer is changed between the bare and Ar covered clusters.

We have tested the effects of some of the theoretical/computational choices which have to be made in order to do calculations on transition metals clusters, including the functional, ECP and basis set, or inclusion of SOC, and found they did not lead to significant changes in the lowest-energy structures for these very small Pt clusters. We have also measured spectra for larger clusters, where our preliminary calculations suggest SOC may become more important in determining the favoured geometry. The good agreement between the calculated spectra of the low-energy isomers and the experimental FIR-MPD spectra for all three sizes suggests that in this size range the TPSS functional recovers the correct lowest-energy structures and that SOC does not change the favoured isomer.

ACKNOWLEDGMENTS

We gratefully acknowledge the support of the Stichting voor Fundamenteel Onderzoek der Materie (FOM) for providing FELIX beamtime and thank the FELIX staff, particularly Dr. A.F.G van der Meer and Dr. B. Redlich, for their skillful assistance. We thank Gerard Meijer for his continued support. This work is funded by the Deutsche Forschungsgemeinschaft through research grant FI893/3-1. DJH thanks the Alexander von Humboldt Foundation for a fellowship.

¹S. Gilb, P. Weis, F. Furche, R. Ahlrichs, and M. M. Kappes, *J. Chem. Phys.* **116**, 4094 (2002).

²J. Li, X. Li, H.-J. Zhai, and L.-S. Wang, *Science* **299**, 864 (2003).

³M. P. Johansson, A. Lechtken, D. Schooss, M. M. Kappes, and F. Furche, *Phys. Rev. A* **77**, 053202 (2008).

⁴P. Gruene, D. M. Rayner, B. Redlich, A. F. G. van der Meer, J. T. Lyon, G. Meijer, and A. Fielicke, *Science* **321**, 674 (2008).

⁵T. Futschek, J. Hafner, and M. Marsman, *J. Phys.: Condens. Mat.* **18**, 9703 (2006).

⁶M. N. Huda, M. K. Niranjana, B. R. Sahu, and L. Kleinman, *Phys. Rev. A* **73**, 053201 (2006).

⁷A. Sebetci, *Chem. Phys.* **331**, 9 (2006).

⁸V. Kumar and Y. Kawazoe, *Phys. Rev. B* **77**, 205418 (2008).

⁹A. Sebetci, *Phys. Chem. Chem. Phys.* **11**, 921 (2009).

¹⁰P. Błoński, S. Dennler, and J. Hafner, *J. Chem. Phys.* **134**, 034107 (2011).

¹¹C. L. Herida, V. Ferraresi-Currotto, and M. B. López, *Comp. Mater. Sci.* **53**, 18 (2012).

¹²D. J. Trevor, D. M. Cox, and A. Kaldor, *J. Am. Chem. Soc.* **112**, 3742 (1990).

¹³U. Achatz, C. Berg, S. Joos, B. S. Fox, M. K. Beyer, G. Niedner-Schatteburg, and V. E. Bondybey, *Chem. Phys. Lett.* **320**, 53 (2000).

¹⁴T. Hanamura, M. Ichihashi, and T. Kondow, *J. Phys. Chem. A* **106**, 11465 (2002).

¹⁵K. Koszinowski, D. Schröder, and H. Schwarz, *J. Phys. Chem. A* **107**, 4999 (2003).

¹⁶I. Balteanu, O. P. Balaj, M. K. Beyer, and V. E. Bondybey, *Phys. Chem. Chem. Phys.* **6**, 2910 (2004).

¹⁷G. Kummerlöwe, I. Balteanu, Z. Sun, O. P. Balaj, V. E. Bondybey, and M. K. Beyer, *Int. J. Mass Spectrom.* **254**, 183 (2006).

¹⁸C. Adlhart and E. Uggerud, *Chem. Commun.*, 2581(2006).

¹⁹C. Adlhart and E. Uggerud, *Chem. Eur. J.* **13**, 6883 (2007).

²⁰K. M. Ervin, J. Ho, and W. C. Lineberger, *J. Chem. Phys.* **89**, 4514 (1988).

²¹D. Dai and K. Balasubramanian, *J. Chem. Phys.* **103**, 648 (1995).

²²D. Majumdar, D. Dai, and K. Balasubramanian, *J. Chem. Phys.* **113**, 7919 (2000).

²³D. Majumdar, D. Dai, and K. Balasubramanian, *J. Chem. Phys.* **113**, 7928 (2000).

²⁴A. Fielicke, A. Kirilyuk, C. Ratsch, J. Behler, M. Scheffler, G. von Helden, and G. Meijer, *Phys. Rev. Lett.* **93**, 023401 (2004).

²⁵A. Fielicke, G. von Helden, and G. Meijer, *Eur. Phys. J. D* **34**, 83 (2005).

²⁶D. Oepts, A. F. G. van der Meer, and P. W. van Amersfoort, *Infrared Phys. Technol.* **36**, 297 (1995).

²⁷J. Tao, J. P. Perdew, V. N. Staroverov, and G. E. Scuseria, *Phys. Rev. Lett.* **91**, 146401 (2003).

²⁸D. Andrae, U. Häußerman, M. Dolg, H. Stoll, and H. Preuß, *Theor. Chim. Acta.* **77**, 123 (1990).

²⁹F. Weigend and R. Ahlrichs, *Phys. Chem. Chem. Phys.* **7**, 3297 (2005).

³⁰R. Ahlrichs, M. Bär, M. Häser, H. Horn, and C. Kölmel, *Chem. Phys. Lett.* **162**, 165 (1989).

³¹M. Valiev, E. Bylaska, N. Govind, K. Kowalski, T. Straatsma, H. V. Dam, D. Wang, J. Nieplocha, E. Apra, T. Windus, and W. de Jong, *Comp. Phys. Commun.* **181**, 1477 (2010).

³²R. B. Ross, J. M. Powers, T. Atashroo, W. C. Ermler, L. A. LaJohn, and P. A. Christiansen, *J. Chem. Phys.* **93**, 6654 (1990).

³³See EPAPS Document No. xxxxxxxxxxxx for details of the calculations for the bare clusters and the MD simulation. For more information on EPAPS, see <http://www.aip.org/pupserve/epaps.html>.

³⁴Spin contamination was a problem for doublet states in both sets of calculations performed without SOC, with $\langle S^2 \rangle$ values suggesting a mix of doublet and quartet states. In some cases we were able to find uncontaminated doublets by changing the orbital occupations, but these had significantly higher energies. In the SOC calculations $\langle S^2 \rangle$ need not be close to $S(S+1)$.

³⁵V. Blum, R. Gehrke, F. Hanke, P. Havu, V. Havu, X. Ren, K. Reuter, and M. Scheffler, *Comp. Phys. Commun.* **180**, 2175 (2009).

³⁶A. Fielicke, C. Ratsch, G. von Helden, and G. Meijer, *J. Chem. Phys.* **127**, 234306 (2007).

³⁷A. Fielicke, P. Gruene, M. Haertelt, D. J. Harding, and G. Meijer, *J. Phys. Chem. A* **114**, 9755 (2010).